Figure S1

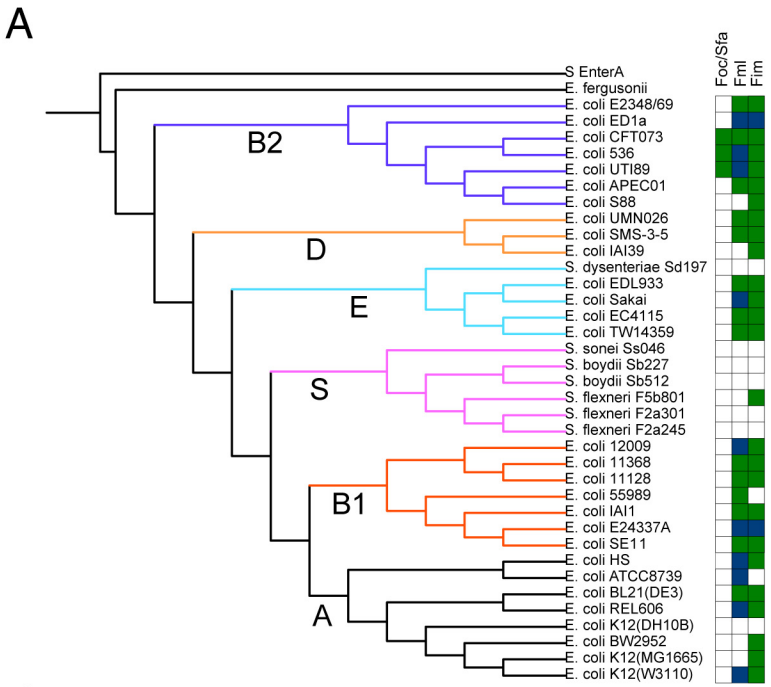
A
Foc/Sfa
Fml
Fim
S EnterA
E. fergusonii
E. coli E2348/69
E. coli ED1a
E. coli CFT073
E. coli 536
E. coli UTI89
E. coli APEC01
E. coli S88
E. coli UMN026
E. coli SMS-3-5
E. coli IAI39
S. dysenteriae Sd197
E. coli EDL933
E. coli Sakai
E. coli EC4115
E. coli TW14359
S. sonei Ss046
S. boydii Sb227
S. boydii Sb512
S. flexneri F5b801
S. flexneri F2a301
S. flexneri F2a245
E. coli 12009
E. coli 11368
E. coli 11128
E. coli 55989
E. coli IAI1
E. coli E24337A
E. coli SE11
E. coli HS
E. coli ATCC8739
E. coli BL21(DE3)
E. coli REL606
E. coli K12(DH10B)
E. coli BW2952
E. coli K12(MG1665)
E. coli K12(W3110)
B2
D
E
S
B1
A

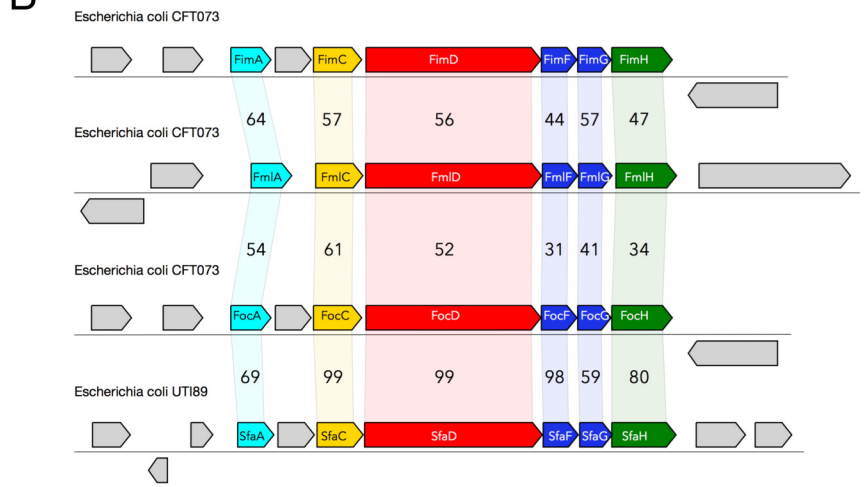
B
Escherichia coli CFT073
FimA
FimC
FimD
FimF
FimG
FimH
64
57
56
44
57
47
Escherichia coli CFT073
FmlA
FmlC
FmlD
FmlF
FmlG
FmlH
54
61
52
31
41
34
Escherichia coli CFT073
FocA
FocC
FocD
FocF
FocG
FocH
69
99
99
98
59
80
Escherichia coli UTI89
SfaA
SfaC
SfaD
SfaF
SfaG
SfaH

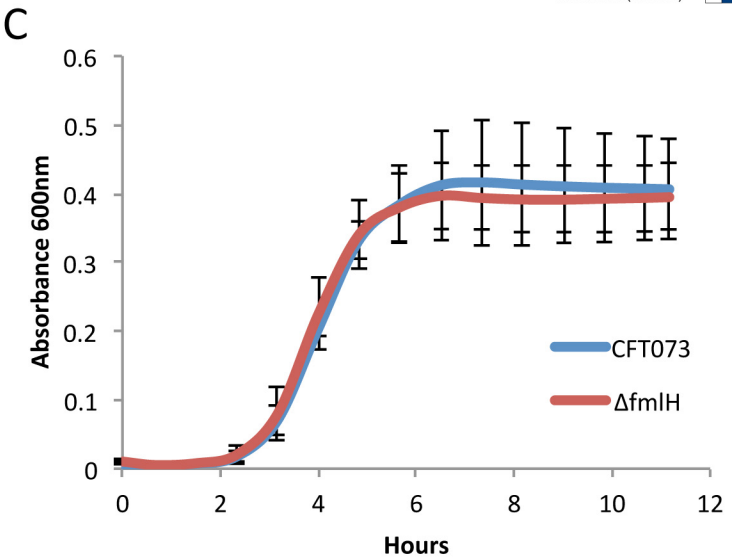
C
Absorbance 600nm
0.6
0.5
0.4
0.3
0.2
0.1
0
0
2
4
6
8
10
12
Hours
CFT073
ΔfmlH

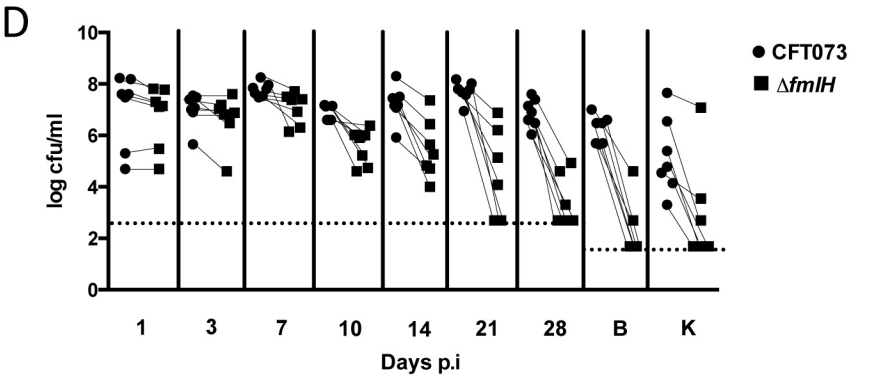
D
log cfu/ml
10
8
6
4
2
0
1
3
7
10
14
21
28
B
K
Days p.i
CFT073
ΔfmlH

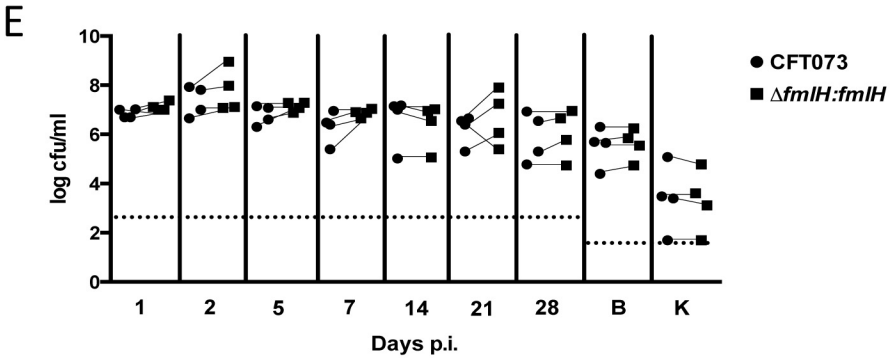
E
log cfu/ml
10
8
6
4
2
0
1
2
5
7
14
21
28
B
K
Days p.i.
CFT073
ΔfmlH:fmlH

Figure S2

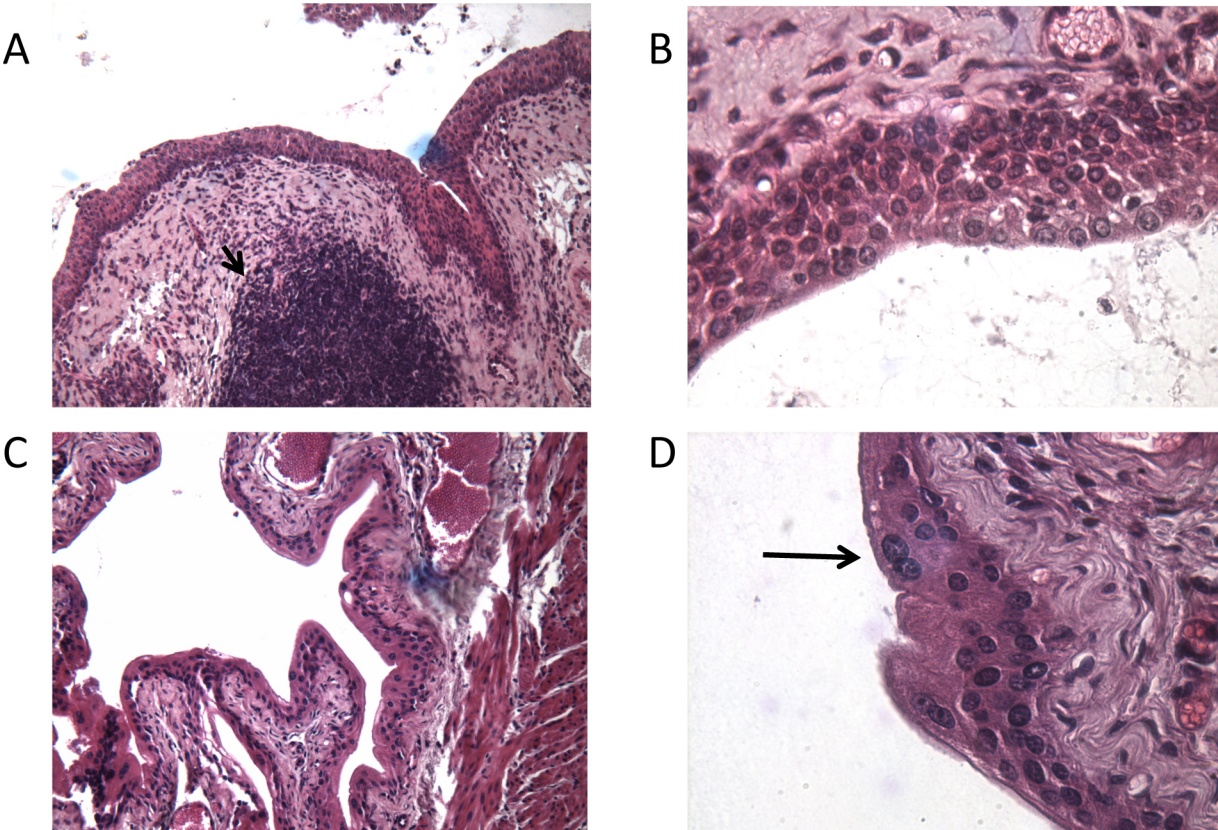

Figure S3

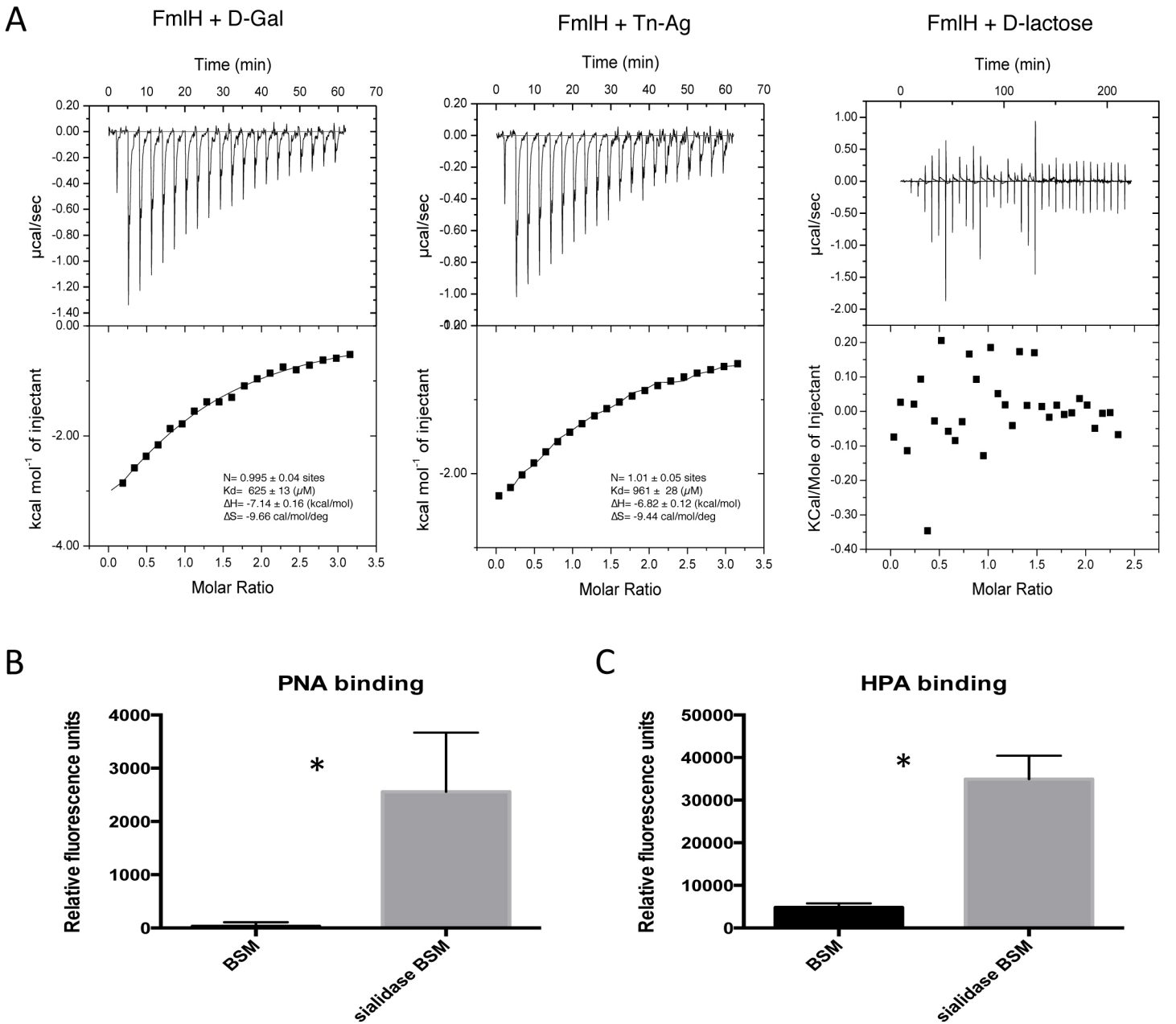
A
FmlH + D-Gal
FmlH + Tn-Ag
FmlH + D-lactose
Time (min)
µcal/sec
kcal mol^{-1} of injectant
KCal/Mole of Injectant
Molar Ratio
N= 0.995 ± 0.04 sites
Kd= 625 ± 13 (µM)
ΔH= -7.14 ± 0.16 (kcal/mol)
ΔS= -9.66 cal/mol/deg
N= 1.01 ± 0.05 sites
Kd= 961 ± 28 (µM)
ΔH= -6.82 ± 0.12 (kcal/mol)
ΔS= -9.44 cal/mol/deg
B
PNA binding
C
HPA binding
Relative fluorescence units
*
BSM
sialidase BSM

Figure S4

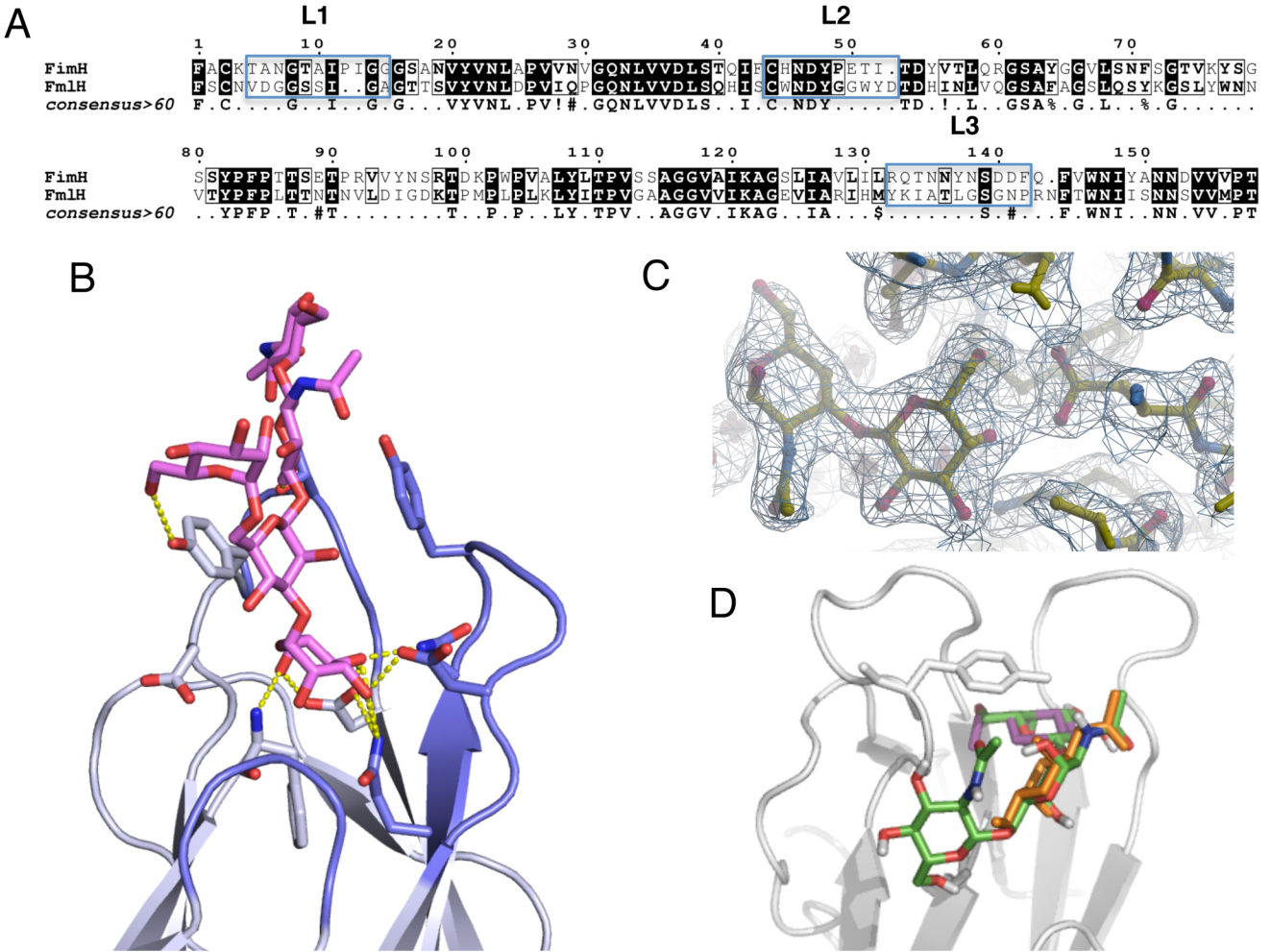

Figure S5

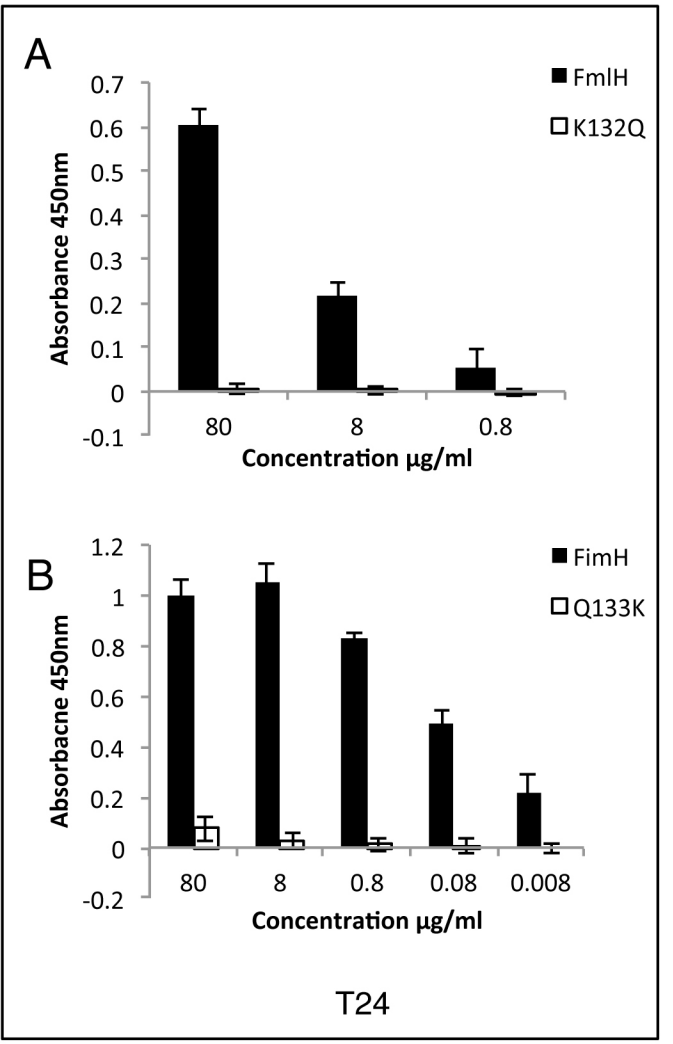
A
FmlH
K132Q
Absorbance 450nm
0.7
0.6
0.5
0.4
0.3
0.2
0.1
0
-0.1
80
8
0.8
Concentration µg/ml
B
FimH
Q133K
Absorbacne 450nm
1.2
1
0.8
0.6
0.4
0.2
0
-0.2
80
8
0.8
0.08
0.008
Concentration µg/ml
T24

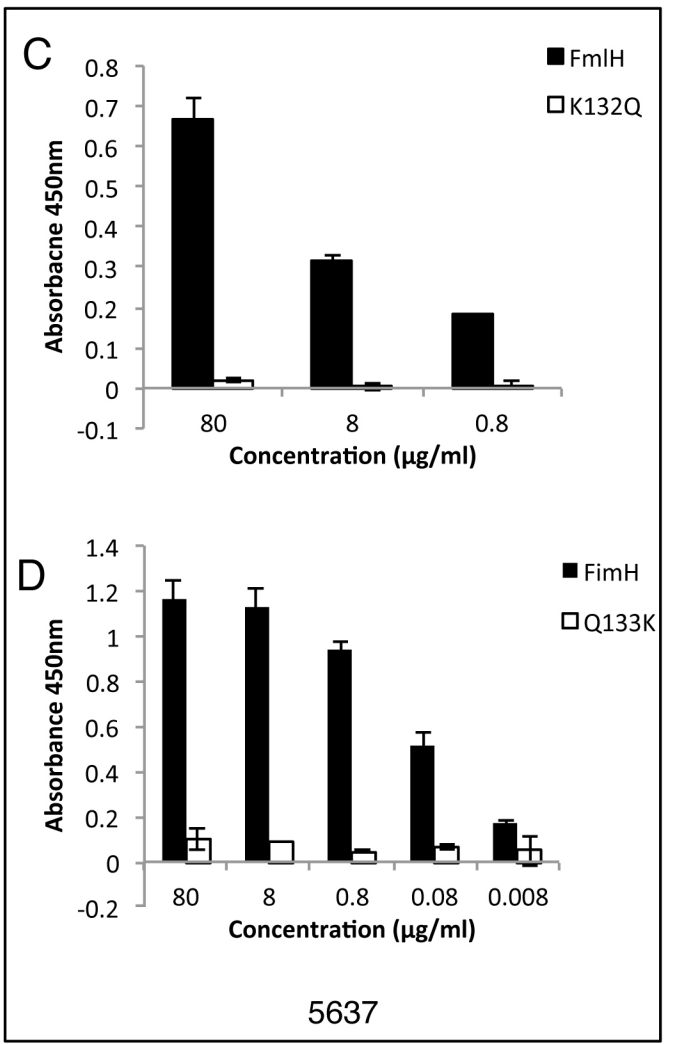
C
FmlH
K132Q
Absorbacne 450nm
0.8
0.7
0.6
0.5
0.4
0.3
0.2
0.1
0
-0.1
80
8
0.8
Concentration (µg/ml)
D
FimH
Q133K
Absorbance 450nm
1.4
1.2
1
0.8
0.6
0.4
0.2
0
-0.2
80
8
0.8
0.08
0.008
Concentration (µg/ml)
5637

Figure S6

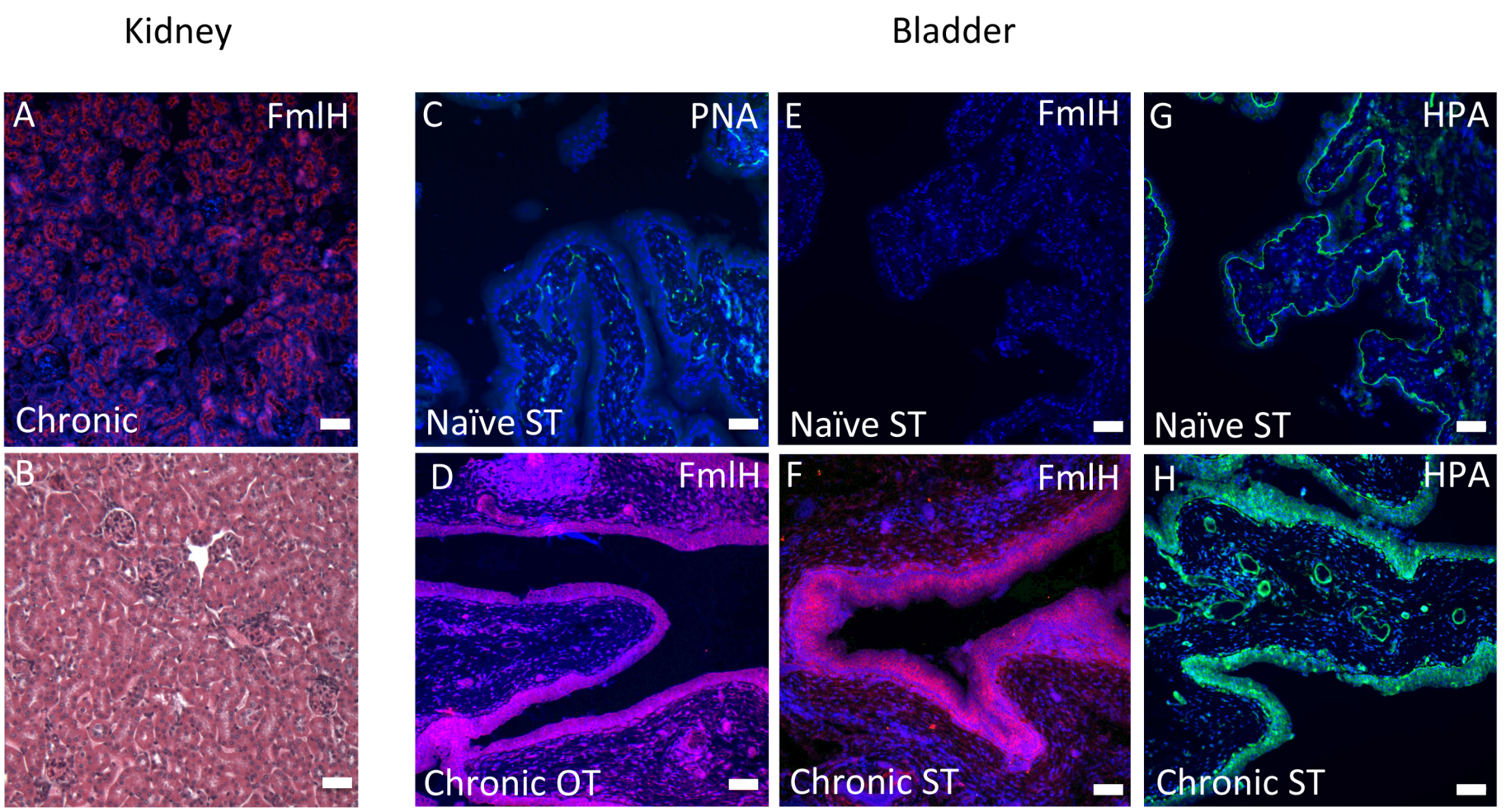
Kidney
Bladder
A
FmlH
Chronic
B
C
PNA
Naïve ST
D
FmlH
Chronic OT
E
FmlH
Naïve ST
F
FmlH
Chronic ST
G
HPA
Naïve ST
H
HPA
Chronic ST

SUPPLEMENTARY FIGURE LEGENDS

Figure S1, related to Figure 1. Fim-related chaperone-usher pili in *E. coli* and *Shigella* **(A)** Distribution of type 1 (*fim*), F1C (*foc*), S (Sfa) and F9 (*fml*) in *E. coli* and *Shigella* genomes. White and green blocks represent absence or presence of the respective gene clusters. Blue blocks represent presence of truncated (likely inactive) gene clusters. **(B)** Comparison of operon structures and percentage amino acid identities between the homologous proteins of pili in the type 1-like cluster of chaperone-usher operons (*fim*, *sfa*, *foc* and *fml*). The F9 cluster in CFT073 contains six genes (*c1931-c1936*), the gene products of which as here referred to as FmlA (F9 major pilin), FmlC (F9 chaperone), FmlD (F9 usher), FmlF and FmlG (F9 minor pilins) and FmlH (F9 adhesin), in accordance with nomenclature of the respective proteins encoded in the F1C, S and type 1 pilus gene clusters. **(C)** Growth comparison between CFT073 and Δ*fmlH*. N=5. **(D, E)** CFU from competitive infections. (D) CFU from competitive infections displayed in Figure 1A and B between CFT073 and *ΔfmlH*, n=7. (E) Bacterial titers from the competitive infections displayed in Figure 1C between CFT073 and *ΔfmlH:fmlH,* n=4.

Figure S2, related to Figure 1. H&E stains of chronic and naïve bladders. (**A** and **B**) Representative images of chronically infected bladders harvest 28dpi, 100X and 400X respectively. Short arrow denotes lymphoid aggregates, not present in (**C** and **D**). (**C** and **D**) Representative images of naïve bladders, 100X and 400X respectively. Long arrow denotes the presence of large terminally differentiated superficial epithelial cells, which are not present in (**A** and **B**).

Figure S3, related to Figure 2. (A) $FmlH^{AD}$ - Gal and - αGalNAc binding thermodynamics**.** ITC injection heats (upper) and normalized binding isotherms (lower) of $FmlH^{AD}$ titrated with D-galactose (left panel), Tn-antigen (N-acetylgalactosamine-α-1-O-serine; middle panel) or D-lactose as control (right panel). $FmlH^{AD}$ binds to Galactose and Tn with an affinity of 625μM and 961μM, respectively, and shows no binding to D-lactose. **(B, C)** HPA and PNA binding to BSM. PNA FITC (B) or HPA Alexa Fluor 488 (C) binding to BSM with or without sialidase treatment. Asterisk denotes $p>0.05$, Mann-Whitney test. Repeated in triplicate, n=6.

Figure S4, related to Figure 3. (A) Pairwise sequence alignment of the FmlH and FimH lectin domains. Conserved residues are highlighted in black. The L1, L2 and L3 loops in the F9 and type 1 receptor binding pockets represent the regions with highest sequence divergence (boxed). **(B)** Ribbon representation of FimH lectin domain structure in complex with Oligomannose-3 (PDB 2VCO). Oligomannose-3 is depicted in stick model and colored pink, red and blue for respectively carbon, oxygen and nitrogen atoms. Hydrogen bonds are depicted in yellow dashed lines. **(C)** 2FoFc electron density contoured 1 σ in the glycan binding pocket of the $FmlH^{AD}$-TF complex. **(D)** Modelled (Autodock Vina (Trott and Olson, 2010)) binding pose of the immature Core 2 trisaccharide (GlcNAcβ1-6(Galβ1-3)GalNAc; colored green, red and blue for carbon, oxygen and nitrogen) in the $FmlH^{AD}$ carbohydrate binding pocket, superimposed with the TF carbohydrate (orange) as found in the $FmlH^{AD}$-TF X-ray structure.

Figure S5, related to Figure 4. ELISA showing FmlH binding to 5637 and T24 cells. **(A&C)** $FmlH^{AD}$ and K132Q or **(B&D)** FimH and Q133K binding to 5637 **(A-B)** or T24 (**C-**

D) urothelial cell lines. Columns represent the mean of each data set and bars represent the standard deviation. Repeated in triplicate, n=3.

Figure S6, related to figure 5. Kidney: **(A)** $FmlH^{ADmC}$ (red) binding to kidneys isolated from chronic cystitis mice. **(B)** H&E stain of representative kidney section indicative of the FmlH and PNA binding regions shown in Figures 4 and S5A. Naïve bladder **(C, E, G)**: PNA (green) (C), $FmlH^{ADmC}$ (red) (E) and HPA (green) (G) staining in naïve bladders after sialidase treatment (labeled ST). Chronic bladder **(D, F, H)**: $FmlH^{ADmC}$ (red) (D) binding to chronically infected bladders after O-glycosidase treatment (labeled OT). $FmlH^{ADmC}$ (red) (F) and HPA (green) (H) staining in chromic bladders after sialidase treatment. Blue represents Hoescht DNA staining in all panels. N=3. Bar= 50µm.

Table S1, related to Figure 2

Receptor	Average RFU	% CV	RB
Galβ1-4GlcNAcβ1-6(Galβ1-3)GalNAcα-Sp8	26484	3	100
Neu5Acα2-6Galβ1-4GlcNAcβ1-3Galβ1-4GlcNAcβ1-6(Galβ1-3)GalNAcα-Sp14	21552	17	81,4
Galβ1-4GlcNAcβ1-6(Galβ1-3)GalNAc-Sp14	13466	14	50,8
GlcNAcβ1-6(Galβ1-3)GalNAcα-Sp8	13424	7	50,7
Galβ1-3GalNAcα-Sp8	12950	4	48,9
GalNAcβ-Sp8	11524	6	43,5
Neu5Acα2-3Galβ1-4GlcNAcβ1-6(Galβ1-3)GalNAcα-Sp14	10028	15	37,9
GlcNAcβ1-β1-4GlcNAcβ1-6(Galβ1-3)GalNAcα-Sp14	8689	8	32,8
Neu5Acα2-6(Galβ1-3)GalNAcα-Sp8	8075	19	30,5
Galβ1-4GlcNAcβ1-3Galβ1-4GlcNAcβ1-6(Galβ1-3)GalNAcα-Sp14	7323	27	27,6
Galβ1-3GlcNAcβ1-6(Galβ1-3)GalNAc-Sp14	7096	31	26,8
Galβ1-3GalNAcα-Sp14	6296	25	23,8
Neu5Acα2-6Galβ1-4GlcNAcβ1-6(Galβ1-3)GalNAcα-Sp14	5980	2	22,6
GlcNAcβ1-6(Galβ1-3)GalNAcα-Sp14	5337	44	20,2
Neu5Acα2-6(Galβ1-3)GalNAcα-Sp14	3695	68	14,0
Neu5Acα2-3Galβ1-4GlcNAcβ1-3Galβ1-4GlcNAcβ1-6(Galβ1-3)GalNAcα-Sp14	2328	4	8,8
Neu5Acα2-3Gal v1-4(Fucα1-3)GlcNAcβ1-6(Galβ1-3)GalNAcα-Sp14	1357	11	5,1
Neu5Acβ2-6(Galβ1-3)GalNAcα-Sp8	933	15	3,5
GalNAcβ1-3Galα1-6Galβ1-4Glcβ-Sp8	378	24	1,4
GalNAcα1-3(Fucα1-2)Galβ1-3GalNAcα1-3(Fucα1-2)Galβ1-4GlcNAcβ-Sp0	365	23	1,4
GalNAcα1-3(Fucα1-2)Galβ1-3GalNAcβ1-3Galα1-4Galβ1-4Glc-Sp21	316	12	1,2
GalNAcβ1-3Galβ-Sp8	298	12	1,1
GalNAcβ1-3Galα1-4Galβ1-4GlcNAcβ-Sp0	212	9	0,8
Galβ-Sp8	209	7	0,8
Galβ1-3GalNAcβ-Sp8	206	23	0,8
Galβ1-6Galβ-Sp10	192	17	0,7
GalNAcα1-3Galβ-Sp8	168	56	0,6
GlcNAcβ1-6GalNAcα-Sp8	109	10	0,4
GalNAcα-Sp8	106	15	0,4
Galβ1-3GalNAcα-Sp16	99	15	0,4

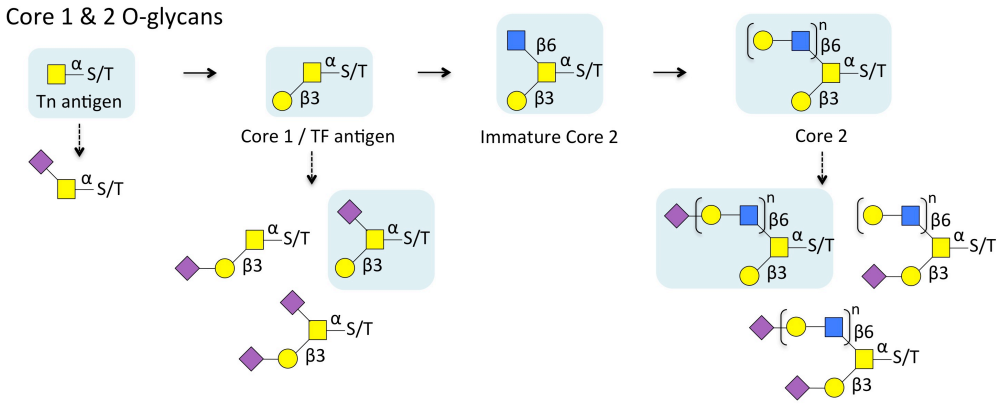

Legend: Top scoring interaction profiles for FmlD^{AD} binding to Version 5.0 of the printed core H array consisting of 611 mammalian glycans (full data are available at functionalglycomics.org under accession code: primscreen_3972). Data are shown as average relative fluorescence units (RFU) (*n*=4); % coefficient of variation (CV; % standard deviation ratio to mean). The top 30 binding profiles are shown, with RB giving the % binding response relative to the strongest binder. Lower panel shows synthesis pathway for Core 1 and 2 O-glycans. Gal, GalNAc, GlcNAc and Neu5Ac are shown as yellow circle and and yellow, blue or magenta squares, respectively.

Table S2, related to Figure 3	**ApoFmlH^{AD}**	**FmlH^{AD}:TF**
Data collection		
Wavelength	0.9795	0.97631
Beamline	i04	i03
Space group	P1	P21 21 2
a, b, c (Å)	52.71, 52.73, 62.82	118.82, 51.46, 53.74
α, β, g (°)	66.9, 82.28, 84.1	90, 90, 90
Resolution range (Å)	57.48-2.09	59.41-2.20
Total reflections	95705	122486
Unique reflections	35660	17285
Rmeas (%)[1]	10.3 (61.6)	5.6 (92.2)
Average I/σI [1]	8.0 (2.1)	10.8 (2.1)
Completeness (%)[1]	97.8 (96.8)	99.6 (97.5)
Multiplicity[1]	2.7 (2.7)	7.1 (6.9)
Wilson B-factor	36.0	39.1
Refinement		
Rwork/Rfree(%)	19.71/ 23.85	18.01/22.45
average B-factor (Å 2)	43.8	36.2
R.m.s. deviations		
Bond lengths (Å)	0.019	0.021
Bond angles (°)	1.846	2.022
No. Atoms (non H)		
Protein	4875	2545
Carbohydrate	-	104
Water	204	81
Ramachandran		
Favoured (%)	96.91	96.36
Allowed (%)	3.09	4.64
Ouliers (%)	0	0
MolProbity score	1.58	1.08
PDB entry	**5LNG**	**5LNE**

Data collection statistics for apo FmlHAD and FmlHAD-TF complex. Data were integrated and scaled using XDS and XSCALE (Kabsch, 2010) and the structures were refined using Refmac 5.5 (The CCP4 suite: programs for protein crystallography., 1994). 1Values for highest resolution shell are given in parentheses.

Table S3, related to Figures 1, 2, 3, 4, 5 and 6. Strains and plasmids.

Strain or plasmid	Description or phenotype[a]	Reference/source
E. coli		
DH5α	*fhuA2 lac(del)U169 phoA glnV44 Φ80' lacZ(del)M15 gyrA96 recA1 relA1 endA1 thi-1 hsdR17*	Lab collection
C43(DE3)	F – *ompT hsdSB (rB- mB-) gal dcm* (DE3)	Lab collection Miroux & Walker, 1996
CFT073::*Cm*	Wild type CFT073 with Cm^R gene integrated into the HK site	Schwartz, 2013
CFT073Δ*fmlH::* Km	CFT073 with Km^R gene inserted into *fmlH*	This study
CFT073Δ*fmlH:fmlH*	Δ*fmlH* strain with *fmlH* integrated into the original deletion site	This study
CFT073Δ*fmlH::* Km p*fmlH*	Δ*fmlH* strain with plasmid p*fmlH*	This study
Cloning plasmids		
pDONR^{TM}221	Gateway® entry vector containing *attP1* and *attP2* sites, Km^R	Invitrogen
pDEST^{TM}14	Gateway® destination vector containing *attR1* and *attR2* sites, T7 promoter, Ap^R, IPTG inducible.	Invitrogen
pTRC99a	Expression vector	
Plasmids		
p*fmlH*^{AD}	*fmlH* lectin domain gene cloned in pDEST^{TM}14, 6xHis tag in C-ter, Ap^R	This study
pSWU19	*Myxococcus* expression vector containing *mCherry* sequence	Sun *et al.* 2011
p*fmlH*^{ADmC}	*fmlH* lectin domain gene fused with mCherry sequence cloned into pDEST^{TM}14, Ap^R	This study
p*fmlH*	*fmlH* cloned into pTRC99a for expression	This study

[a] Ap^R, ampicillin resistance; Km^R, kanamycin resistance; Cm^R, Chloramphenicol resistance

Table S4 Primers, related to Figures 1, 2, 3, 4, 5 and 6

	Oligonucleotides (5’-3’)[a]
Gene engineering/cloning	
FmlD lectin domain	
FmlH-1	GGGGACAAGTTTGTACAAAAAAGCAGGCTTAAGAAGGAGATATACCATGGGTAAAACATTCAGTATAAAGGTCCTGT
FmlH-2	GGGGACCACTTTGTACAAGAAAGCTGGGTATTA**GTGGTGATGGTGATGGTG**TGTTGGCATAACAACACTGTTATTTGA
fmlH full length 5'	GGGGTACCCCATGGGTAAAACATTCAGTATAAAGGTCC
fmlH full length 3'	GCTCTAGAGCTTATTCATAGATAAAAGTGACACC
mCherry sequence	
FmlH-3	TTATTTCAAATAACAGTGTTGTTATGCCAACAGGTGGCGTGAGCAAGGGCGAGGAGGATAACATGGCCAT
mCherry5’	TTATTTCAAATAACAGTGTTGTTATGCCAACAGGTGGCGTGAGCAAGGGCGAGGAGGATAACATGGCCAT
mCherry3’	GGGGACCACTTTGTACAAGAAAGCTGGGTATTACTTGTACAGCTCGTCCATGCCGCCGGTGGAGTGGCGG
qPCR	
C1galt1 5'	CTTTGGGCGAAGATTTAAGC
C1galt1 3'	GATGGAAGGTTTCTTTCCCA
Ggta1 5'	TCTACCACGGGAGTGTGTGT

Ggta1 3'	GTCCTCATCGTCAGCTGTGT
B4galnt1 5'	GGATTATCCACCACCACCTC
B4galnt1 3’	AAGAGGATATGGCTCCATCG
B3gnt3 5'	CTTCGAGATGCTGCTGATGT
B3gnt3 3’	TGCCCTATGAACTCCTCAGA
Galnt3 5'	CTCGTAACCAAGTTCGCCTT
Galnt3 3’	ACGCTTCCGGGTAAATAGTG
Galnt4 3'	ACGTGTGATGCCCTTGATAA
Galnt4 5’	TGCTCTGTGTACCCAGCTTC
GyrA qPCR 5'	GACAGAAGACTCTTTAAAGCGCAC
GyrA qPCR 3'	GGTACCGTGAAGAAAACTGTCCTC
FmlA qPCR 5'	GTATCGTCATTACTGGTGACAGTAG
FmlA qPCR 3'	GAATCAATGAACCAAACGGTTGAGC
FimI qPCR 5'	GCCGCTGATAAACAAATGACGGTC
FimI qPCR 3'	CACATCCGGATTTTTACCATCCGC

Chromosomal* fmlD *manipulation

FmlH KO 5'	ATGGGTAAAACATTCAGTATAAAGGTCCTGTTCGGTATTTATCTTCTATTCATATGAATATCCTCCTTAG
FmlH KO 3'	TTATTCATAGATAAAAGTGACACCAATGACTGACTGGACGGCTCCGGCTGGTGTAGGCTGGAGCTGCTTC
FmlH rein 5'	ATGGGTAAAACATTCAGTATAAAGGTCCTGTTCGGTATTTATCTTCTATT
FmlH rein 3'	TTATTCATAGATAAAAGTGACACCAATGACTGACTGGACGGCTCCGGCTG

Site directed mutagenesis

K132Q 5'	CGTATTCATATGTATCAAATTGCCACGTTAGGAAGCG
K132Q 3'	CGCTTCCTAACGTGGCAATTTGATACATATGAATACG
D53E 5'	GCTGGTACGACACTGAGCATATAAACCTGGTAC
D53E 3'	GTACCAGGTTTATATGCTCAGTGTCGTACCAGC
D53K 5'	GCTGGTACGACACTAAACATATAAACCTGGTAC
D53K 3'	GTACCAGGTTTATATGTTTAGTGTCGTACCAGC

---

[a] *attB recombination* sites have been underlined in sequence. His-tag is shown in bold letters.

SUPPLEMENTAL INFORMATION

EXTENDED EXPERIMENTAL PROCEDURES

Attachment assays- 100µg of BSM in PBS was dried to Immulon 4HBX 96 well plates overnight at room temperature (RT). BSM coated wells were then treated with sialidase, 0.01 U/ml, for 1h at 37^{o}C or mock treated with PBS. Plates were blocked with 1% BSA for 1h at RT. Wells were incubated with biotinylated FmlH^{AD} protein, or ~1*10^{7} CFU of CFT073, *ΔfmlH* or *ΔfmlH*pfmlH for bacterial binding assays. Plates were then washed 4 times with 0.05% Tween in PBS (PBST) and incubated with Streptavidin conjugated to horseradish peroxidase (1:200) or rabbit anti-*E.coli* antibody (1:1000) and subsequently goat anti-rabbit HRP conjugated antibody (1:2000) in 1% BSA for 1h at RT before washing. 100µl of tetramethylbenzidine (TMB) was added and the reaction was stopped with 50µl of 1M sulfuric acid. Background values were determined from mock treated wells and subtracted from the experimental wells for normalization. Absorbance was quantified using a Molecular Devices plate reader at 450nm. Experiments were repeated in triplicate with each experiment including 4 technical replicates.

Similarly, FITC labeled PNA (Sigma L7381) and HPA Alexa Fluor 488 (Life Technologies L11271) were allowed to attach to BSM or sialidase treated BSM at a 1:100 concentration. After washing, relative fluorescence was quantitated using a Tecan Infinite M200 Pro.

RNA extraction and qPCR- Chronically infected bladders were homogenized in Trizol upon extraction from the mouse. This solution was then further lysed by bead beating with .1mm silica beads for 1 min, twice. RNA extraction was then performed using the Zymo Research Direct-zol RNA mini-prep kit per the manufactures instructions. RNA extractions for bacterial inoculum (2x24) cultures were performed similarly. Samples were DNase treated before reverse transcription as described previously. qPCR was performed with cDNA utilizing the Syber Green system (BioRad) to determine Ct values which were then used to calculate relative fold change using the commonly used ΔΔCt method(Khetrapal et al., 2015). *gapdh* and *gyrA* were utilized for standardizing host and bacterial expression profiles, respectively. Values are representative of expression patterns measured from 3 PBS and/or 5 chronically infected mice. The same mice were utilized for both host and bacterial transcript samples.

Primers for qPCR analysis are listed in Table S4. *fimI* was chosen as a representative of the fim locus due to primer incompatibility issues within *fimA* (Conover et al., 2016; Greene et al., 2014).

FmlH lectin domain purification- The first 158 amino acids of FmlH were cloned into pDEST14 using Gateway® technology (Invitrogen) with a 6 His tag incorporated into the C terminus, resulting in plasmid p*fmlH*^{AD}. Expression was induced with 0.1mM IPTG. Periplasm extracts were prepared by resuspending bacterial pellets in 4mls of 20mM Tris, 20% sucrose pH 8 per gram of cell pellet. 40µl of 0.5M EDTA and 10mg/ml lysozyme per gram of cells was added to this suspension and incubated on ice for 30 minutes. Next, 40µl of 2.5M $MgCl_2$ was added per gram of cells and incubated on ice for 5 minutes. Cells were spun at 15,000x g and the supernatant was saved as the periplasmic extract. The periplasm containing FmlH lectin domain was then dialyzed against 1XPBS and run over a Cobalt (Goldbio) column and eluted with 1XPBS/200mM

Imidazole. Pooled fractions containing FmlH lectin domain were dialyzed against 20mM Tris pH 8.4 and run over a Source 15Q eluted at 100mM NaCl.

FmlH mCherry fusion construction- To engineer a His-tagged $FmlH^{AD}$ mCherry fusion protein ($FmlH^{ADmC}$) under the control of the IPTG-inducible T7 promoter, the *fmlH* sequence was amplified from *E.coli CFT073* genomic DNA using the oligonucleotide pair FmlH-1/FmlH-3 and the *mCherry* sequence was amplified from pSWU19 plasmid using mCherry5'/mCherry3' oligonucleotides (Table S3) (Sun et al., 2011). The resulting DNA fragments were used as template for an overlapping PCR with FmlH-1/mCherry3' oligonucleotides. The resulting DNA fragment was inserted using Gateway® technology (Invitrogen) into the pDEST14. The corresponding vector was named p$fmlH^{ADmC}$.

FmlH point mutant construction- By utilizing p$fmlH^{AD}$ as a template, primers were designed for quick-change mutagenesis of target sites (table S4). Following the PCR reaction, products were Dpn1 digested to remove the plasmid template. Purified products were transformed into C43(DE3) and/or C600 cells for expression and purification using Ni-NTA agarose.

Crystallization and structure determination- Prior to crystallization, the His-tagged $FmlH^{AD}$ was dialyzed into 20mM Tris-HCl pH 8, 1M NaCl. His-tagged $FmlH^{AD}$ (8mg mL^{-1}) was crystallized using sitting drop vapor diffusion against a solution containing 0.1M Citrate pH2, 1M Ammonium sulfate. For co-crystallization, His-tagged $FmlH^{AD}$ (24mg mL^{-1}) was incubated with 1mM Thomsen-Friedenreich glycan (TF: Galß1-3GalNAc) (Lectinity, Russia), and crystallized in 0.1M Citrate pH2, 2.2M ammonium sulfate, 20% glycerol. $FmlH^{AD}$ crystals were flashed cooled to 100K in crystallization buffer, cryoprotected with Paratone-N. Data for apo $FmlH^{AD}$ and $FmlH^{AD}$:TF were collected at beamline i04 (DIAMOND, United Kingdom) to a resolution of 1.75 and 2.2 Å, respectively. Data were indexed and processed with XDS and Xscale (Kabsch, 2010), phased by molecular replacement [Phaser (Collaborative Computational Project, 1994)] using coordinates of FimH (PDB:2VCO) and refined using Refmac5.5 (The CCP4 suite: programs for protein crystallography., 1994). Crystal parameters and data processing statistics for the all structures are summarized in Table S2.

Surface Plasmon Resonance (SPR) measurements. Surface plasmon resonance experiments were carried out using a Biacore 3000 instrument (GE healthcare). For TF affinity measurement, the surface of a CM5 sensor chip (GE healthcare) was activated with 0.05 M N-hydroxysuccinimide (NHS) and 0.2 M 1-ethyl-3-(3-dimethylaminopropyl) carbodiimide hydrochloride (EDC). After activation of the surface, the glycoconjugate TF-APE-human serum albumin (Galβ1-3GalNAcα1-O-APE-HSA) in 10 mM sodium acetate pH 4, was immobilized on the sensor surface via primary amine groups present on human serum albumin. An equivalent amount of human serum albumin was immobilized in the control channel. Residual unreacted active ester groups were blocked with 1 M ethanolamine-HCl, pH 8.5. The sensor chip and $FmlH^{AD}$ were equilibrated in HBS buffer (10mM HEPES, 150mM NaCl, 1mM EDTA, 0.005% Tween20, pH 7.4). $FmlH^{AD}$ was then flowed over the chip surface in a concentration series ranging 140 nM to 144 µM at a flow rate of 20 µL min^{-1} at 25°C and dose-response curves were acquired by plotting steady state resonance units (RU) against $FmlH^{AD}$ concentration. Regeneration of the sensor surface between measurements was done by extended washing in HBS buffer.

For Core2 affinity measurement, the biotinylated core 2 glycan ((GlcNAcβ1-6(Galβ1-3)GalNAc-poly[N-(2-hydroxyethyl)acrylamide]-$(CH2)_6$-biotin); Lectinicity) was immobilized on a streptavidin (SA) sensor chip (GE healthcare). $FmlH^{AD}$ was flowed over the chip surface with concentrations ranging 140 nM to 144 μM in HBS buffer at a flow rate of 20 μL min^{-1} at 25°C and dose-response curves were acquired by plotting steady state RU against $FmlH^{AD}$ concentration. Regeneration of the sensor surface between measurements was done by extended washing in HBS buffer.

Data were evaluated using the software BIAeval (Biacore AB). The control-subtracted equilibrium signals were plotted versus input $FmlH^{AD}$ concentrations, and a Langmuir binding isotherm with a 1:1 stoichiometry was fitted to the normalized dose-response curves to derive the dissociation constant (Kd) (Prism).

Isothermal titration calorimetry (ITC)-ITC measurements were performed on a MicroCal iTC200 calorimeter (Malvern). $FmlH^{AD}$ (439μM) was loaded into the cell of the calorimeter and the D-Galactose (D-Gal), Tn-Antigen (DGalNAc-α-1-O-Ser; Sigma-Aldrich) or D-Lactose were loaded in the syringe at 6.5 mM concentration. All measurements were done at 25°C, with a stirring speed of 300 rpm and performed in 20 mM Tris buffer (pH 8). Binding data were analyzed using the MicroCal LLC ITC200 software.

Tissue staining- Urinary tract tissues harvested from naïve or chronically infected mice were fixed with methacarn and processed into paraffin blocks for sectioning and slide preparation. After antigen retrieval, slides were deparaffinized with two 5 min washes with xylene followed by rehydration with 2 washes in isopropanol. Samples were then rinsed with water for 5 min. Next, slides were boiled for 30 min in 10mM sodium citrate and then allowed to cool to RT. Sections were blocked for 1h in 1%BSA PBST. $FmlH^{ADmC}$ was diluted 1:100 in the blocking solution and allowed to bind the tissues for 1h. Samples were then washed 3 times with PBS followed by Hoechst staining, 1:20,000 for DNA visualization. Additional staining with HPA and PNA FITC conjugated lectins were performed similarly at a 1:500 dilution. Enzymatic treatment with O-glycosidase or alpha-N-Acetyl-galactosaminidase (NEB) were performed at 37°C in the supplied buffer per the manufacturer's instructions (Koutsioulis et al., 2008; Wong-Madden and Landry, 1995). Slides were then examined using a Zeiss Axioskop 2 microscope.

Cell line binding- 5637 and T24 cells were grown to 80-90% confluence in T-25 flasks in RPMI media supplemented with 10% fetal bovine serum at 37°C and 5% CO_2. Cells were split using trypsin digestion and seeded at an concentration of ~$2x10^5$ cells per ml into 24 well plates containing sterilized 12mm round glass coverslips for overnight attachment. Cells were allowed to grown and attach to the coverslips overnight at 37°C and 5% CO_2. The next day, cells were fixed with 4% paraformaldehyde for 15min at RT. Coverslips were then blocked with 1% BSA PBS for 1h at RT. FmlH was diluted into the 1% BSA PBS at 100μg/ml with 300μl being added to each well and allowed to bind for 1h at RT. Wells were washed 3X with PBS for 5 min with gentle shaking. Mouse anti-FmlH sera was then added in 1%BSA PBS at a concentration of 1:5000 for 1h at RT followed by washing as before. Anti-mouse sera conjugated to Texas red was added at 1:1000 for 1h at RT followed by washing and staining with Hoechst staining. Coverslips were then removed from the wells and mounted on slides with prolong anti-fade reagent. Slides were then examined using a Zeiss Axioskop 2 microscope.

Urine protein concentration- 300ml of normal human urine was collected and centrifuged to remove contaminating cells. Total protein was then precipitated with 40% ammonium sulfate overnight at 4^{o}C. Precipitate was then collected by centrifugation and resuspended in 4-5ml of PBS. Solution was then dialyzed against PBS and analyzed using coomassie stained SDS-PAGE. ELISA assay were performed on the concentrate similarly as with BSM. Human urine collection was performed with informed consent and approved under IRB 201207143.

Growth Curves- Overnight cultures of CFT073 or Δ*fmlH* were diluted 1:1000 in LB and dispensed into 96 well plates in 100µl aliquots. Optical density 600nm was measured every 50 minutes over 12hrs in a Tecan Infinite M200 Pro at 37^{o}C.

Far Western blotting- Urine concentrates were separated by SDS-PAGE and transferred to PVDF. Membranes were blocked overnight in 5% milk TBST. FmlH lectin domain was added to the 5% milk TBST for a final concentration of 3µg/ml and allowed to incubate for 1h followed by washing 3X with TBST for 5 min. Mouse anti-FmlH was added in 5% milk TBST at a concentration of 1:2000 for 1h at RT. Following washing, 1:4000 rabbit anti-mouse HRP antibody was added for 1h. Detection using Super Signal West Femto (Thermo Scientific) was performed after a final wash.

SUPPLEMENTRAL REFERENCES

Khetrapal, V., Mehershahi, K., Rafee, S., Chen, S., Lim, C.L., and Chen, S.L. (2015). A set of powerful negative selection systems for unmodified Enterobacteriaceae. Nucleic Acids Res *43*, e83.

Conover, M.S., Hadjifrangiskou, M., Palermo, J.J., Hibbing, M.E., Dodson, K.W., and Hultgren, S.J. (2016). Metabolic Requirements of Escherichia coli in Intracellular Bacterial Communities during Urinary Tract Infection Pathogenesis. mBio *7*.

Greene, S.E., Pinkner, J.S., Chorell, E., Dodson, K.W., Shaffer, C.L., Conover, M.S., Livny, J., Hadjifrangiskou, M., Almqvist, F., and Hultgren, S.J. (2014). Pilicide ec240 disrupts virulence circuits in uropathogenic Escherichia coli. mBio *5*, e02038.

Koutsioulis, D., Landry, D., and Guthrie, E.P. (2008). Novel endo-alpha-N-acetylgalactosaminidases with broader substrate specificity. Glycobiology *18*, 799-805.

Sun, M., Wartel, M., Cascales, E., Shaevitz, J.W., and Mignot, T. (2011). Motor-driven intracellular transport powers bacterial gliding motility. Proceedings of the National Academy of Sciences of the United States of America *108*, 7559-7564.

Trott, O., and Olson, A.J. (2010). AutoDock Vina: improving the speed and accuracy of docking with a new scoring function, efficient optimization, and multithreading. J Comput Chem *31*, 455-461.

Wong-Madden, S.T., and Landry, D. (1995). Purification and characterization of novel glycosidases from the bacterial genus Xanthomonas. Glycobiology *5*, 19-28.